International Journal of Applied Science-Research and Review
ISSN: 2394-9988

Open Access Research Article

CO_2 hydrogenation to methane over Zeolite promoted Ni/CeO_2 Catalysts at Atmospheric Pressure

Abdullahi Isah*

Department of Science Laboratory Technology, Umaru Ali Shinkafi Polytechnic, Sokoto, Nigeria

ABSTRACT

The zeolite promoted Ni/CeO_2 catalysts were constructed *via* impregnation method and applied for conversion of CO_2 to methane at atmospheric pressure for the first time. The influence of calcination temperatures and operation conditions (such as reaction temperature, Gas Hourly Space Velocity (GHSV), H_2/CO_2 ratio) were studied. The results uncovered that the non-promoted 10 wt% Ni/CeO_2 catalyst showed $\%CO_2$ conversion and $\%CH_4$ selectivity (about 99% CO_2 conversion and 35.5% CH_4 selectivity) and the zeolite (2-8 wt%) promoted 10 wt% Ni/CeO_2 catalysts recorded (about 99% CO_2 conversion and 0-17.6% CH_4 selectivity) at 350 atmospheric pressure, gas hourly space velocity (GHSV) of 72000 SmL $(gcat\ h)^{-1}$ and the H_2/CO_2 ratio of 4. The zeolite promoter addition to 10 wt% Ni/CeO_2 clearly and significantly reduced the $\%\ CH_4$ selectivity and this selectivity reduction is directly proportional to the quantity of the zeolite added. The physicochemical characterizations of the catalysts in terms of morphology, compositional phase, functional group, Brunauer Emmett Teller (BET) surface area (m^2/g), total volume (m^3/g), mesoporous volume (m^3/g), average pore diameter (A), Ni metal surface area, average crystallite size (nm) were carried out with Scanning Electron Microscope (SEM), X-Ray Diffract meter (XRD), Fourier Transform Infrared spectrophotometer (FTIR), Brunauer Emmett Teller surface area analyzer, Debye-Scherrer equation, BJH method.

Keywords: CO_2 methanation; Zeolite promoter; Ni/CeO_2 based catalysts

INTRODUCTION

As a result of the growing human population and their activities, the use of fossil fuels is dramatically increasing consequently the proportion of the atmospheric carbon dioxide is rising continuously [1-4]. Considering Carbon Dioxide (CO_2) a chief Greenhouse Gas (GHG) hence one of the main agents of global warming and a key player to climate change [5,6]. Nowadays became one of the dominants environmental concerns of the present century faced by human race [7,8]. As such, there is an urgent universal demand to arrest the global warming caused by the accumulation of carbon dioxide in the atmosphere thereby providing lasting solutions to this issue [9]. Therefore, one of the encouraging techniques to mitigate anthropogenic CO_2 from the atmosphere is carbon capture utilization and this makes the area an interesting for the researchers [10]. Catalytic hydrogenation of carbon dioxide has been investigated as one of the suitable approaches for the recycling of CO_2 to valuable substances especially when hydrogen is readily available from the renewable sources such as hydrolysis of water [11-16]. The Sabatier reaction known as methanation reaction found to be one of the suitable catalytic hydrogenation of carbon dioxide. This methanation reaction as reported in the equation (1) and (2) is a process in which methane is generated from hydrogen and carbon dioxide or

Received:	02-April-2022	**Manuscript No:**	IPIAS-22-12812
Editor assigned:	05-April-2022	**PreQC No:**	IPIAS-22-12812 (PQ)
Reviewed:	19-April-2022	**QC No:**	IPIAS-22-12812
Revised:	10-October-2022	**Manuscript No:**	IPIAS-22-12812 (R)
Published:	17-October-2022	**DOI:**	10.36648/2394-9988.9.12.101

Corresponding author Abdullahi Isah, Department of Science Laboratory Technology, Umaru Ali Shinkafi Polytechnic, Sokoto, Nigeria; E-mail: wang760612@126.com

Citation Isah A (2022) CO_2 hydrogenation to methane over Zeolite promoted Ni/CeO_2 Catalysts at Atmospheric Pressure. Int J Appl Sci Res Rev. 9:101.

Carbon monoxide (CO) or even CO_2/CO mixture and the key component for this process is found to be the catalysts design. Recently, numerous methanation catalysts such as Co, Fe, Mo, Ni and Ru dispersed over support ZrO_2, TiO_2, SiO_2, CeO_2 and Al_2O_3 due to their high catalytic activity and selectivity as such have gotten considerable attention [17].

$CO_{2(g)}+4H_{2(g)} \rightarrow CH_{4(g)}+2H_2O_{(g)} (\Delta H_{298}=-165$ kj/mol) (1)

$CO_{(g)}+3H_{2(g)} \rightarrow CH_{4(g)}+H_2O_{(g)} (\Delta H_{298}=-206$ kj/mol) (2)

This paper reported the addition of zeolite promoter to the 10 wt% Ni/CeO_2 and 10 wt% Ni/Al_2O_3 catalysts and evaluated for CO_2 hydrogenation to methane at atmospheric pressure for the irst time. The support (ceria) and promoter (zeolite) used in this work have relative lower cost compared to support (alumina) used in the commercial catalyst as such, using ceria as a support and incorporation of such zeolite promoter will signi icantly reduce the cost of the catalyst production and expect to have better catalytic performance and catalytic stability than the commercial catalyst.

MATERIALS AND METHODS

Analytical grade ≥ 99% nickel nitrate hex hydrate (Merck), 98% aluminium oxide (Sigma Aldrich), 98% cerium dioxide (Sigma Aldrich), 98% zeolite (Sigma Aldrich) and distilled water produced using Sartorius 61316 and 611 UV ultrapure water system (UK) were used for the synthesis of the catalysts. Liquid CO_2 (>99.99%), 10% CH_4 in Ar (>99.99%) and H_2 (>99.99%) all purchased from from Linde Group company were used for the catalytic reaction.

Synthesis of Catalysts

The catalysts of non-promoted 10 wt% Ni/CeO_2 (NC) and 10 wt% Ni/CeO_2 promoted with various zeolite weight percentage (NZC-X) were synthesized *via* impregnation method. The Ni/CeO_2/zeolite weight percentage is 10/90/0 for NC, the concentration of Ni is ixed at 10 wt% where X varied (2-8 wt%). Brie ly, for NC and NZC-X catalysts, 0.99 g Ni $(NO_3)_2.6H_2O$ was weighed and dissolved in 20 mL distilled water to form an aqueous solution. Then 1.80 g of cerium (IV) oxide (ceria) for NC, 1.76 g of cerium (IV) oxide (ceria) and 0.04 g of zeolite for NZC-2 was added slowly with constant stirring to the aqueous solution. The obtained slurry was dried at 110°C in an oven for 12 hours. All the dried catalyst samples were mixed thoroughly and then calcined in a muffle furnace at 400°C for 4 hours. Only NC was further calcined at different temperatures (350-500°C) for calcination experiments.

Characterization of the Catalysts

The determination of the structural morphology of each catalyst was carried out using Scanning Electron Microscope (SEM). Each catalyst was coated with a thin layer of gold by a sputter coater and then examined at an accelerating voltage of 40 kV with JSM-6510 SEM (JEOL Ltd). The X-Ray Diffraction (XRD) analysis of the catalysts was determined using an ARL X'TRA X-ray Diffract meter (thermo scienti ic) at a scanning speed 12°/minute over the 2θ range of 20-70°. The XRD was operated with a Ni filtered Cu Ka radiation source at 40 kV and 40 mA. The identification of the compositional phases was carried out by comparing with the Joint Committee on Powder Diffraction Standards (JCPDS). The average size (μm) of the catalysts was 54 obtained from the SEM images using image application. The crystallite size of the catalysts (D) was calculated using the XRD data and the Scherer's equation [18].

$$D=\frac{k\lambda}{\beta\cos\theta}$$

where, K is the shape factor (0.94), λ is X-ray wavelength (0.154 nm), β is the line broadening at half the maximum intensity in radians (FWHM), and θ is Bragg angle. Fourier transform infrared (FT-IR) spectra were recorded in the wavelength range of 400-4000 cm^{-1} using an IR prestige-21 FT-IR Spectrophotometer (Shimadzu). The Brunauer Emmett Teller (BET) surface area, total pore volume, Mesoporous volumes, average pore diameter and the Ni metal surface area determined by AutoSorb-6iSA instrument
(Quanta chrome) at -196°C using N_2 adsorption-desorption measurements.

Catalytic Testing

The catalytic performance of each catalyst was studied under atmospheric pressure in a continuous low ixed bed reactor with a catalytic bed of 5 mm (inner diameter) and 20 mm length. The reactor was placed horizontally in a muffle furnace equipped with a temperature control unit. The introduction of all gases into the reactor were monitored and controlled by calibrated mass low meters. Before the catalytic performance test, 250 mg of each calcined catalyst was sandwiched between two layers of glass wool in the catalytic bed and then pretreated (reduced) with pure hydrogen gas for 2 hours using a total gas low of 100 mL/min with a heating rate of 10°C/min up to 400°C and then cooled down to the speci ic reaction temperature (250-450°C). A terwards, a mixture of H_2 and CO_2 gas with a molar ratio of 4 (H_2:CO_2) was introduced into the reactor at a low rate of 300 mL/min, under atmospheric pressure. A ter 1 hour of reaction the irst sample was taken in duplicate.
The outlet gas samples were analyzed using Gas Chromatography Mass Spectrophotometry (GCMS-TQ8040, Shimadzu, Japan) equipped with a carboxen-1010 plot capillary column (30 m × 0.32 mm, Supelco Sigma-Aldrich).
Each of the reaction temperatures was maintained for 30 minutes before the next temperature was adjusted and each experiment was conducted in duplicate. The catalytic conversion and product selectivity were calculated as follows using equation 3 and 4, respectively Cco_2 (mol.$L^{-1}s^{-1}$) and Cco_2 (out) (mol.$L^{-1}s^{-1}$) where are the concentrations of CO_2 entering and exiting the reactor respectively.

$$CO_2\ Conversion\ (\%) = \frac{C_{CO_2(in)} - C_{CO_2(out)}}{C_{CO_2(in)}} x100 \quad (3)$$

$$CH_4\ Selectivity\ (\%) = \frac{C_{CO_2\ converted\ to\ CH_4}}{C_{CO_2(in)} - C_{CO_2(out)}} x100 \quad (4)$$

Based on the repeated experiments, the variability in the CO_2 conversion and CH_4 selectivity are estimated to be within ± 0.79% and ±7.7%, respectively.

RESULTS AND DISCUSSION

Texture, Structure and Morphological Characteristics

Figure 1 illustrates the SEM images of the samples. The micrographs showed that the size of the smaller particles within the samples increased consistently from NC to NZC-8. This increase in small particle sizes could not be unconnected to the addition of zeolite promoter to Ni/CeO_2. The NC exhibited a relative higher surface area in comparison to NC zeolite promoted catalysts.

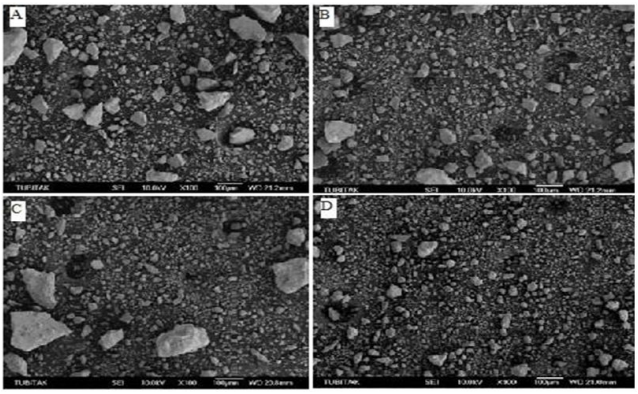

Figure 1: SEM images of (A) NC; (B) NZC-2; (C) NZA-4; (D) NZA-8 catalysts claimed at 400°C.

The XRD patterns are displayed in **Figure 2**. The characteristic peaks at 2θ indicated that the 8 wt% of zeolite addition to Ni/CeO_2 catalyst slightly shifted the NiO and CeO_2 peaks to lower 2θ values. The 2θ values for NC are NiO (36.88, 43.13 and 62.63, JCPDS 22–1189) and CeO_2 (28.38, 33.13, 47.19, 56.19, 58.88, 69.38, 76.88 and 79.06) while that of NZC-8 are NiO (36.75, 42.88 and 62.50) and CeO_2 (28.25, 32.80, 47.13, 56.13, 58.75, 69.00, 76.56 and 79.00, JCPDS81-0792 which is clear indication that the higher zeolite content changed the lattice constant of the Ni/CeO_2. Hence, the superior catalytic performance of NC can be attributed to the strong synergistic effects between finely dispersed NiO species and oxygen vacancies in CeO_2. More so, the surface coverage by CO_2 derived species on the CeO_2 support contributed to the outstanding performance of NC. The Scherer's equation gives the average crystallite size of 16.37 nm, 15.81 nm, 15.68 nm and 15.39 nm for NC, NZC-2, NZC-4 and NZC-8, respectively (**Figure 2**).

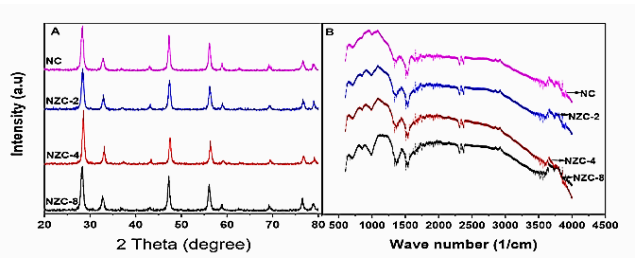

Figure 2: (A) XRD patterns of NC, NZC-2, NZC-4 and NZC-8 catalysts; (B) FT-IR spectra of NC, NZC-2, NZC-4 and NZC-8 catalysts.

Figure 2 depicts the infrared absorption peaks of the samples. The obvious absorption peaks of zeolite at 3568 cm^{-1}, 1689 cm^{-1} and 994 cm^{-1} are attributed to the structural O-H, physically absorbed water and bending vibration peaks of Si–O, respectively [19]. The broad band at 3335–3786 cm^{-1} in all the spectra is attributed to the stretching vibration of -OH. The peaks below 1000 cm^{-1} are related to metal oxides (NiO) from the interatomic vibrations. Bonds observed at 1435 and 1690 cm^{-1} corresponded to the physically adsorbed water molecule and hydroxyl group. The spectra of the zeolite promoted nano catalysts (NZC-2, NZC-4 and NZC-8) show the characteristic peak of zeolite (994 cm^{-1}), with a slight displacement and decrease in intensity. The specific surface areas (BET), pore volumes and areas covered by the Ni metal of the samples are listed in **Table 1**. As obtained from the image software, all the samples have particles size below 100 nm with an average particle size of 47.52 nm, indicating a nano sized particle. In comparison with NC, specific surface areas of NZC-X obviously decreased. This is attributed to the integration of zeolite particles (with an average surface area of (m^2/g)) on the NZC-X, resulting in increased particle dispersion and 200–700 nm porosity. Notably, both the pore volume and BET surface area of NZC-X exhibited a decreasing trend with increasing the zeolite concentration. This may be due to the gradual degradation of the zeolite structure during the calcination. Also, the slight decreased in crystallite sizes (XRD data) could also be due to the degradation of zeolite at calcinations of 400°C and can result in the decreasing trend of BET surface area (m^2/g) and pores volume of NZC-X. The NC has the highest specific surface area (82.3 m^3/g), consistent with its better catalytic performance than the 24 pore volume (0.273 cm) other nano catalysts (**Table 1**).

Table 1: Textural characteristics of the Ni/CeO_2 based catalysts claimed at 400°C.

Catalyst	Code name	BET[a] (m^2/g)	$V_{total\ ab}$ (m^3/g)	$V_{meso\ ac}$ (m^3/g)	D (A°)[c]	Ni metal S_A	ACS[d] (nm)
Ni/CeO_2	NC	82.3	0.273	0.154	48.2	2.96	16.37
Ni/2 wt% zeo/CeO_2	NZC-2	73.5	0.141	0.094	56.8	2.43	15.81

Ni/4 wt% zeo/CeO_2	NZC-4	65.5	0.109	0.083	49.9	2.29	15.68
Ni/10 wt% zeo/CeO_2	NZC-8	56.4	0.093	0.071	28.9	1.85	15.39

D: Average pore diameter; V_{Total}: Total pore volume, V_{meso}: Mesoporous volume,

[a] Determined by BET equation, [b] Determined by single point adsorption, [c] Determined by the BJH method, [d] Determined by Debye-Scheerer equation; ACS: Average Crystallite Size (nm); Ni metal S_A: Ni metal surface area; zero=zeolite

The Influence of Reaction Temperature

The results shown in **Figure 3** revealed that the reaction temperature did not have significance influence on the catalytic CO_2 conversion. All the non-promoted 10 wt% Ni/CeO_2 and zeolite promoted 10 wt% Ni/CeO_2 catalysts (NC, NZC-2, NZC-4, NZC-8) showed very high (~99%) CO_2 conversion percentage at the reaction temperatures tested (250-450°C). Such high CO_2 conversion values were obtained with nickel supported ceria catalysts on previously reported in other study. The influence of the reaction temperature on CH_4 selectivity was clearly observed in **Figure 4**. At low reaction temperatures up to 300°C, all the catalysts including NA showed a very low CH_4 selectivity. The highest CH_4 selectivity of 68% and 35.5% were achieved for NA and NC at 350°C respectively. When the reaction temperature was increased, NA sustained a similar CH_4 selectivity at 400°C and 43% at 450°C, while CH_4 selectivity decreased to almost zero at a temperature between 400-450°C for NC. The CH_4 selectivity of all the zeolite promoted 10 wt% Ni/CeO_2 (NZC-2, NZC-4 and NZC-8) were almost zero at reaction temperature of 250-300°C. At 350°C the selectivity was almost zero for NZC-8, 8% for NZC-2 and 17% for NZC-4. Similarly, at 400-450°C the NZC-4 and NZC-8 reported almost no CH_4 formation, while NZC-2 exhibited 17.5% and 11.0% CH_4 selectivity at 400 and 450°C respectively. There was no CO formation for any of the catalyst investigated at all the reaction temperatures tested, similar to what was observed elsewhere. It is obvious that the addition of zeolite does not promote the CH_4 selectivity rather lower the selectivity. The lower CH_4 selectivity reported by promoted catalysts might be due to the lower BET surface area (m^2/g), Ni metal surface area (1.85-2.43 m^2/g), total volume (0.093-0.141(56.4-C73.5 mm^3/g) and meso volume (0.071-0.094 m^3/g) when compared to that of NC (82.3 m^2/g, 2.93 m^2/g, 0.273 m^3/g and 0.154 m^3/g respectively) as shown in **Table 1**. The reduced CH_4 selectivity as the proportion of zeolite increased might be connected with less availability of Ni metal surface area as well as consistent decreased in the BET surface area. Hence, the superior catalytic performance of NC can be attributed to the strong synergistic effects between finely dispersed NiO species and oxygen vacancies in CeO_2. More so, the surface coverage by CO_2 derived species on the CeO_2 support contributed to the outstanding performance of NC. Despite the lowest BET surface area of 56.4 m^2/g displayed by the NZC-8 still has a comparable CO_2 conversion efficiency with NZC-4 and NZC-2 and this might be due to the fact that the relative higher oxygen storage capacities o f NZC-2 a nd NZC-4 i n CeO_2 compensated their larger particle sizes.

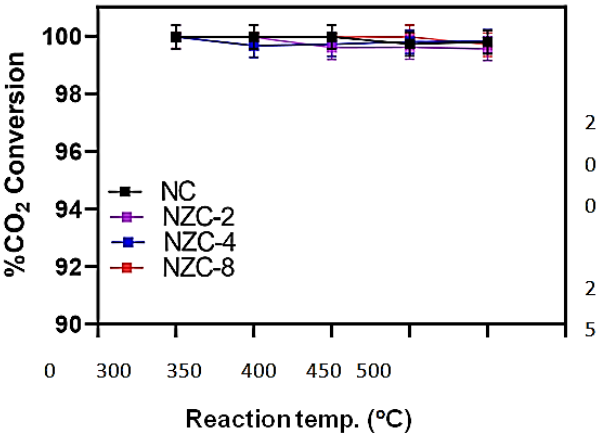

Figure 3: Effect of reaction temperature on $\%CO_2$ conversion of the catalysts (NC, NZC-2, NZC-4, and NZC-8) under atmospheric pressure (1 atm), H_2/CO_2 ratio of 4, GHSV=72000 SmL $(gcat.h)^{-1}$ and calcination temperature of 400°C.

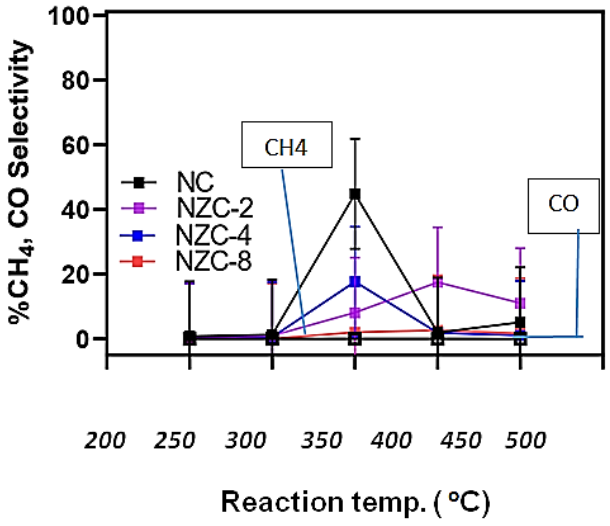

Figure 4: Effect of reaction temperatures on $\%CH_4$, %CO selectivity of the catalysts (NC, NZC-2, NZC-4, NZC-8) under atmospheric pressure (1 atm), H_2/CO_2 ratio of 4, GHSV=72000 SmL$(gcat.h)^{-1}$ and calcination temperature of 400°C.

The influence of calcination temperature and process parameters NC showed the highest methane selectivity, as such, further optimization experiments were conducted using NC. The results indicated that the CO_2 conversion of NC was not influenced by the variations in the temperature at which the catalyst was calcined. Similarly, variation in H_2/CO_2 ratio

and gas hourly space velocity did not affect the CO_2 conversion percent as shown in **Figure 5**, respectively. Neither the reaction parameters nor the catalyst calcination temperatures tested showed any CO_2 selectivity. The results in demonstrated similar CO_2 conversion percentages for NC calcined at various temperatures between 350 and 500°C. Nevertheless, the calcination temperature influenced the methane selectivity of the catalyst. The highest CH_4 selectivity of 35.3% was recorded when NC was calcined at 400°C. When higher calcination temperatures were used, there was a considerable reduction of methane selectivity to 20.5% at 450°C and 21.5% at 500°C. This higher selectivity for NC at calcination temperature 400°C is possibly due to the larger nickel dispersion as well as the formation of smaller NiO crystallite particles on CeO_2. At higher calcination temperatures the Ni is expected to move to the bulk from the surface of the catalyst leading to a stronger Ni-CeO_2 bond, hence adversely affecting the catalytic activity. When the H_2/CO_2 ratio was varied between 3 and 10, the CH_4 selectivity of 35.5% was found to be optimum at the H_2/CO_2 ratio of 4 which is in line with the stoichiometric molar ratio of H_2/CO_2 in the methanation reaction presented in equation 1. The lower or higher H_2/CO_2 ratio than 4 resulted in lower CH_4 selectivity and this is mainly due to the fact that one reacting species (CO_2 or H_2) is limiting while the other in excess. The lowest GHSV of 72000 SmL (gcat h^{-1}) selectivity. This is due to the fact that the contact time between the reacting gases and the catalyst surface is relatively long when compared to the higher GHSV tested. The longer contact time increased the effective collision between the reactants on the catalyst surface, hence resulting in the highest %CH_4 selectivity. As such, to improve the single pass conversion it is necessary to maintain the optimum GHSV as any further increase or decrease in GHSV decreases the %CH_4 selectivity (**Figure 5**).

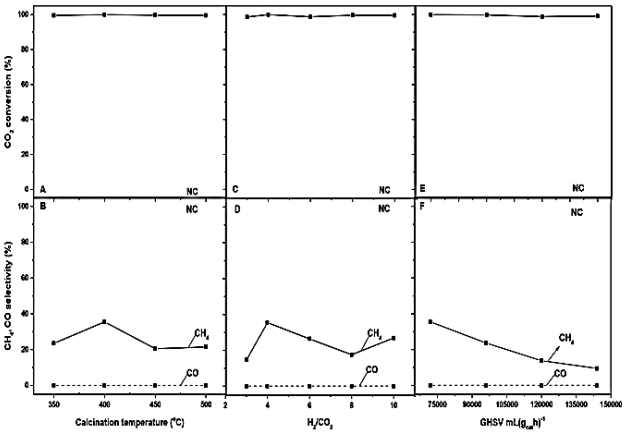

Figure 5: The influence of calcination temperature on a) CO_2 conversion %; b) CH_4; CO selectivity (%) at H_2/CO_2 ratio of 4 and GHSV 72000 SmL (gcat $h)^{-1}$. The influence of H_2/CO_2 ratio on; c) CO_2 conversion %; d) CH_4, CO selectivity (%) with calcination temperature of 400°C and GHSV 72000 SmL (gcat $h)^{-1}$. The influence of GHSV on; e) CO_2 conversion %; f) CH_4, CO selectivity (%) with H_2/CO_2 ratio of 4 and calcination temperature of 400°C. All the experiments were conducted on 10 wt% Ni/CeO_2 under atmospheric pressure and at a reaction temperature of 350°C.

CONCLUSION

All the catalysts investigated recorded significant CO_2 conversion (>99%) at reaction temperature of 250-450°C. The 10% Ni/CeO_2 catalyst recorded the highest CH_4 selectivity of 35.3% at a reaction temperature of 350°C, which may be attributed to the higher BET surface area, total volume, meso volume as well as Ni metal surface area. While the zeolite promoted catalysts exhibited lower CH_4 selectivity in which the catalyst with 8 wt% zeolite recorded almost 0% CH_4 selectivity at all the reaction temperatures investigated. This lower CH_4 selectivity of the zeolite promoted catalysts may not be unconnected with the decreased in the physical characteristics of the catalysts (BET surface areas, total volumes, meso volumes as well as Ni metal surface areas) and decreased in the quantity of CeO_2. The methane selectivity of NC was reduced when the catalyst was calcined at a temperature above 400°C. The reaction temperature of 350°C, H_2/CO_2 ratio of 4 and the GHSV of 72000 SmL (gcat $h)^{-1}$ were found to be the optimum conditions favoring the highest methane selectivity. Ni/CeO_2 shows potential as a low cost catalyst and further optimization studies are required to enhance the methane selectivity and stability.

ACKNOWLEDGEMENT

The Ph.D. research of Abdullahi Isah was funded by the Tertiary Education Trust Fund (TETFUND) provided by the Federal Government of Nigeria. The authors thank Tarık Haydar from the state laboratory based in Cyprus for helping with the Gas Chromatography Mass Spectrometer (GC-MS) analysis of the gas samples.

REFERENCES

1. Kharaji AG, Shariati A (2013) Performance of Co-Mo/Al_2O_3 Nano Catalyst for CAMERE Process in a Batch Reactor. Chem Biochem Eng Q. 27(3):275–278.
2. Li MMJ, Zeng Z, Liao F, Hong X, Tsang SCE (2016) Enhanced CO_2 hydrogenation to methanol over CuZn nanoalloy in Ga modified Cu/ZnO catalysts. J Catal. 343(1):157-167.
3. Abanades JC, Alvarez D (2003) Conversion Limits in the Reaction of CO_2 with Lime. Energy Fuels. 17(2):308–315.
4. Abu-Zahra MRM, Niederer JPM, Feron PHM, Versteeg GF (2007) CO_2 Capture from Power Plants Part II. A Parametric Study of the Economic Performance based on Mono-Ethanolamine. Int J Greenh Gas Con. 1(1):135–142.
5. McCollum D, Bauer N, Calvin K, Kitous A, Riahi K (2014) Fossil resource and energy security dynamics in conventional and carbon-constrained worlds. Clim Change. 123(1):413–426.
6. Yannopoulos SI, Lyberatos G, Theodossiou N, Li W, Valipour M, et al. (2015) Evolution of water lifting devices

(pumps) over the centuries worldwide. Water. 7(9):5031–5060.

7. Valipour M (2012) Comparison of surface irrigation simulation models: full hydrodynamic, zero inertia, kinematic wave. J Agric Sci. 4(12):1-4.
8. Bansode A, Urakawa A (2014) Towards full one-pass conversion of carbon dioxide to methanol and methanol-derived products. J Catal. 309(1):66-70.
9. Bansode A, Tidona B, Von Rohr PR, Urakawa A (2013) Impact of K and Ba promoters on CO_2 hydrogenation over Cu/Al_2O_3 catalysts at high pressure. Catal Sci Technol. 3(1):767-778.
10. Stangeland K, Kalai D, Li H, Yu Z (2022) CO_2 methanation: The effect of catalysts and reaction Conditions. Energy Procedia. 105(1): 2022–2027.
11. Yang C, Ma ZY, Zhao N, Wei W, Hu TD, et al. (2006) Methanol synthesis from CO_2 rich syngas Methanol synthesis from CO_2 rich syngas over a ZrO_2 doped CuZnO catalyst. Catal Today. 115(1):222–227.
12. Li C, Yuan X, Fujimoto K (2014) Development of highly stable catalyst for methanol synthesis from carbon dioxide, Appl Catal. A: General. 46(1):306-311.
13. Jun K, Shen W, Lee K (1999) Concurrent Production of Methanol and Dimethyl Ether from Carbon Dioxide Hydrogenation: Investigation of Reaction Conditions Bull. Korean Chem Soc. 20:993-998.
14. Yu KM, Curcic I, Gabrielm J, Tsang SCE. Recent advances in CO_2 capture and utilization. Chem Sus Chem. 1(11):893-899.
15. Turner J, Sverdrup G, Mann MK, Maness P, Kroposki B, et al. (2007) Renewable hydrogen production. Int J Energy Res. 32(5):379-407.
16. Gao J, Liu Q, Gu F, Liu B, Zhong Z, et al. (2015) Recent advances in methanation catalysts for the production of synthetic natural gas. RSC Adv. 5(1):22759-22776.
17. Patterson A (1939) The Scherrer Formula for X-Ray Particle Size Determination. Phys Rev J Arch. 939(56): 978–982.
18. Talkhoncheh SK, Haghighi M, Jodeiri N, Aghamohammadi S (2017) Hydrogen production over ternary supported Ni/Al_2O_3 clinoptilolite CeO_2 nanocatalyst CH_4/CO_2 reforming: Influence of support composition. J Nat Gas Sci Eng. 46(1):699–709.
19. Oladipo AA, Vaziri R, Abureesh MA (2018) Highly robust $AgIO_3$/MIL (Fe) nanohybrid composites for degradation of organ phosphorus pesticides in single and binary systems: Application of artificial neural networks modelling. J Taiwan Inst Chem Eng. 83(1):133–142.